Energy Proceedings
Vol 60, 2025
ISSN 2004-2965

# Assessment of Heat Extraction and Fracture Behavior in Abandoned Reservoirs#

Zhipeng Wang [1, 2*], Yuanxin Zhang [3], Qidi Cheng [3]

1 State Key Laboratory of Petroleum Resources and Prospecting, China University of Petroleum (Beijing), Beijing 102249, China

2 Department of Chemical and Petroleum Engineering, University of Calgary, Calgary, Alberta T2N1N4, Canada
3 Xinjiang Oil Field Company, Xinjiang 834000, China

(Corresponding Author: zwang_cup@163.com)

**ABSTRACT**

Geothermal development in abandoned reservoirs with $CO_2$ recirculation aligns with energy-transition goals, yet more efficient system designs are needed. This study reconfigures multi-stage fractured horizontal well patterns into a fractured closed-loop geothermal system (FCLG), in which injection–production fractures interconnect to create multiple rows of high-conductivity channels for heat extraction. We build numerical models to compare a conventional closed-loop system (CLG), a conventional multi-stage fractured horizontal well system (MSFHW), and the proposed FCLG, and we obtain dynamic fracture conductivity from core displacement experiments under geothermal conditions. The multiphysics simulations reveal three characteristic production stages for FCLG: an initial plateau, a decline, and a secondary plateau. Sensitivity analysis indicates injection temperature governs heat-extraction efficiency most strongly, followed by injection flow rate and temperature difference; lower injection temperatures, lower flow rates, and larger temperature differences improve performance. Relative to MSFHW, FCLG delivers ~1.7× higher heat-extraction efficiency, ~3× longer stable production, a maximum produced-fluid temperature increase of 12.5–19.9 K, and a maximum net thermal-power gain of 8.9–9.4 MW. Even a single-fracture FCLG (SFCLG) outperforms CLG, achieving 2.27× higher efficiency, a 5.5–16.4 K rise in peak produced temperature, and a 2.25–3.6 MW increase in maximum net heat power. These results demonstrate that the FCLG concept and accompanying models can substantially enhance geothermal recovery from abandoned reservoirs, offering a robust framework for high-efficiency energy applications.

**Keywords:** geothermal heat extraction； evolving fractures；closed-loop fractured network

## 1. INTRODUCTION

Driven by the depletion of fossil resources and worsening environmental pollution, demand for clean energy continues to rise [1–5]. Geothermal energy, a clean and renewable resource, can support residential heating, power generation, and other applications [6–11]. At present, circulating a working fluid to extract heat from geothermal reservoirs is regarded as the most effective approach [12, 13]. In practice, however, efficient development typically requires drilling geothermal wells and carrying out reservoir stimulation via fracturing, along with ongoing monitoring of reservoir parameters—costs that erode project economics [14–17]. Repurposing abandoned reservoirs and their existing well patterns that possess geothermal potential offers a pathway to reduce these costs substantially [18, 19]. Such reservoirs have already undergone drilling, fracturing, and parameter testing; engineers mainly need to retrofit the injection and production wells to suit geothermal extraction. Enabling convenient, efficient, and economical heat recovery from abandoned reservoirs is therefore essential.

Multiple exploitation configurations can be adapted to such retrofits [20–24]. The classic injection–production (IP) system injects a cool fluid through an injector and recovers the heated fluid from a producer to harvest geothermal energy [17, 25]. This scheme works best in formations with moderate to high porosity and permeability; in tight reservoirs, its heat-extraction efficiency is poor. To address this limitation, an injection–production system augmented with fractures (IP-F) has been proposed to enhance performance in low-permeability settings.

In this work, we introduce a fractured closed-loop geothermal (FCLG) system composed of an injection horizontal well, a production horizontal well, and

# This is a paper for the 11th Applied Energy Symposium: Low Carbon Cities & Urban Energy Systems (CUE2025), July 18-22, 2024, Kitakyushu, Japan.

multiple hydraulic fractures connecting them. The injected fluid flows through these fractures to mine heat before being produced at the outlet well. Compared with a closed-loop geothermal (CLG) system, a single-well single-circulating-gas with fracture network (SWSCG-FN) system, a single-well single-circulating-gas (SWSCG) system, and a conventional IP system, the FCLG configuration provides a markedly larger circulating-fluid volume; it also exceeds the IP-F system slightly in circulating volume. Meanwhile, fluid loss in FCLG is far lower than in IP-F and only slightly higher than in SWSCG-FN—still acceptable because flow mainly follows the horizontal wellbores and fractures. To quantify these effects, we establish numerical models for the CLG, multi-stage fractured horizontal well (MSFHW), and FCLG systems and compare their heat-extraction performance. The models are solved with COMSOL Multiphysics 6.1. Core displacement experiments under geothermal reservoir conditions yield a dynamic conductivity function, which is embedded in both the temperature transient analysis models and the numerical models to represent the influence of dynamic fractures on heat recovery. Key parameters in the temperature transient analysis and numerical frameworks are then subjected to sensitivity analysis to assess their impact on performance.

## 2. METHODOLOGY

### *2.1 Experimental apparatus and procedure*

To capture the evolution of dynamic fractures, core-flood experiments were performed on tight sandstone at geothermal reservoir temperatures using $CO_2$ as the displacing fluid. The tests characterize fracture conductivity under reservoir-relevant conditions. The setup comprises a drying oven, muffle furnace, air compressor, constant-flow pump, constant-temperature bath, core holder, back-pressure pump, and a scanning electron microscope. Operating limits are: maximum confining pressure 50 MPa, maximum flow pressure 30 MPa, muffle-furnace temperature up to 1373.15 K, and injection flow rates from 0.1 to 5 mL $min^{-1}$. Pressure is measured with 0.001 MPa accuracy. All experimental data are logged to a computer to ensure continuous, reliable acquisition.

Over four days, cores with artificial fractures undergo pretreatment. First, twelve cores are dried at 378.15 K for 24 h. They are then heated in the muffle furnace to 478.15 K, held for 1 h, and cooled to ambient; this cycle is repeated three times. A water jet removes particles from the fracture surfaces, after which the cores are dried for an additional 24 h. Determination of the dynamic-fracture conductivity function takes 2–3 days per run. $CO_2$ of 99.999% purity is first compressed in an intermediary vessel using a gas-pressurization unit, then delivered to the core holder by a constant-flow pump. The core holder is placed in a constant-temperature chamber so the entire system remains at the geothermal reservoir temperature of 478.15 K. The conductivity function is evaluated by varying temperature, confining pressure, flow rate, and axial pressure. A single experiment spans one week. In total, testing across the twelve cores required 40 days.

### *2.2 Experimental results*

Fig. 1 summarizes the outcomes. Four variables—temperature difference, confining pressure, flow rate, and axial pressure—were varied to assess their effects on the pressure differential. When temperature increased from 400 K to 480 K, the pressure differential rose monotonically; the fitted trend indicates a direct proportionality with slope α (Fig. 1a). Increasing confining pressure from 2.5 MPa to 22.5 MPa likewise produced a consistent rise in pressure differential, with proportionality coefficient β; notably, β exceeds α (Fig. 1b). As the flow rate was raised from 1 mL $min^{-1}$ to 5 mL $min^{-1}$, the pressure differential increased at an accelerating pace, and the fit suggests an exponential dependence characterized by coefficient γ (Fig. 1c). In contrast, changes in axial pressure did not lead to an increase in the pressure differential (Fig. 1d).

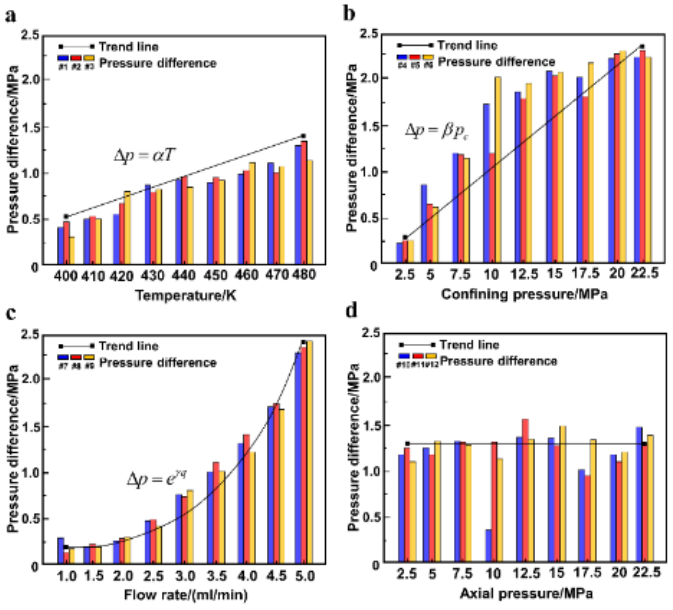


*Fig. 1. Pressure difference varies with changes in temperature difference, confining pressure, flow rate, and axial pressure*

## 3. DISCUSSION

### *3.1 Comparison of numerical simulation results for the GEE-CLG and GEE-SFCLG models*

To benchmark against a conventional closed-loop geothermal (CLG) system, the proposed fractured closed-loop concept was simplified to a single-fracture configuration (SFCLG). A grid-independence study and time-step selection showed that an ultra-fine mesh combined with a 150-hour time step offers the best computational efficiency without sacrificing accuracy for the GEE-SFCLG simulations. Parameters for the subsequent sensitivity analysis were then specified accordingly. The key distinction between CLG and SFCLG lies in the heat-transfer pathway: CLG relies on a horizontal wellbore, whereas SFCLG employs hydraulic and dynamic fractures that traverse the reservoir. Owing to their thin apertures and extensive areal coverage, fractures provide superior heat-exchange performance relative to wellbores, and their direct contact with the circulating fluid minimizes thermal losses otherwise incurred across the reservoir–wellbore–fluid system. When the injection temperature is reduced from 308.15 K to 298.15 K, SFCLG retains its characteristic three-stage production behavior—an initial descent, a transition, and a stable plateau—with a less pronounced temperature drop during the descent. For both CLG and SFCLG, lowering the injection temperature increases the maximum production-temperature difference, reaching 5.5 K at an injection temperature of 298.15 K. Across all cases, CLG yields lower net thermal power than SFCLG; moreover, the maximum net-power advantage of SFCLG widens as the temperature difference grows, amounting to 2.25 MW at a 70 K difference and 3.6 MW at 80 K. Practically, reducing injection temperature enables sustained high net thermal power during geothermal extraction. Varying injection flow rate further highlights the benefit of fractures: at identical flow rates, SFCLG achieves a maximum produced-fluid temperature that is 16.4 K higher and a maximum net thermal power that is 3.2 MW greater than CLG. Overall, the SFCLG configuration delivers a heat-extraction efficiency approximately 2.27 times that of the conventional CLG system.

### *3.2 Numerical simulation results of the GEE-MSFHW models*

The multi-stage fractured horizontal well (MSFHW) configuration is the most prevalent arrangement in oil and gas production and is frequently present in abandoned reservoirs suitable for reuse. For geothermal application, a grid-independence check and time-step assessment identified an ultra-fine mesh combined with a 150-hour time step as an efficient and accurate numerical setup for the GEE-MSFHW model. Parameter ranges for sensitivity analysis were defined accordingly. Structurally, the MSFHW system consists of an injection well, a production well, dynamic fractures, hydraulic fractures, and natural fractures. In hydrocarbon development, the two fracture sets are indirectly connected through natural fractures to expand the sweep and improve recovery. In geothermal service, however, the natural-fracture corridors impede fluid circulation and thus diminish heat-extraction efficiency.

Simulations over a 5000-day period show that the production-temperature trajectory separates into three stages: an initial stable-production stage, a transition stage, and a subsequent stable-production stage. Lowering the injection temperature reduces the produced temperature; a 10 K decrease in injection temperature yields a maximum produced-temperature drop of 21.2 K. The net thermal power over the same period follows the same three-stage behavior. As the produced-temperature difference increases from 70 K to 80 K, the net thermal power rises, with a maximum increase of 1.82 MW. Increasing the injection flow rate leads to gradual declines in both produced temperature and net thermal power; the largest observed decreases correspond to a 16.5 K reduction in produced temperature and a 1.5 MW reduction in maximum net thermal power.

### *3.3 Comparison of numerical simulation results for models GEE-MSFHW and GEE-FCLG model*

The fractured closed-loop geothermal (FCLG) system directly links dynamic fractures with hydraulic fractures, enabling smooth fluid transport from the injector to the producer and promoting efficient heat transfer. Numerical setup choices mirror those used for the MSFHW case: a grid-independence check supports an ultra-fine mesh, and a 150-hour time step provides accuracy with good efficiency. Parameter ranges for sensitivity analysis are predefined on this basis. The fundamental distinction between FCLG and MSFHW is the direct interconnection of fractures in the former, as opposed to the indirect linkage characteristic of the latter. In geothermal service, FCLG markedly outperforms MSFHW. While the produced-temperature behavior in FCLG still exhibits three stages—stable production, transition, and a subsequent stable production—the duration of the stable-production stage is extended by multiples relative to MSFHW. The largest

produced-temperature difference between the two systems is 12.5 K, occurring at the point where the FCLG produced temperature drops sharply. Under temperature differences of 70 K and 80 K, the maximum net heat-power advantages of FCLG over MSFHW are 8.9 MW and 9.4 MW, respectively. Across all conditions, the overall maxima for produced-temperature difference and net heat-power difference reach 19.9 K and 9.1 MW. In aggregate, FCLG delivers roughly 1.7× higher heat-extraction efficiency and about 3× longer stable heat-extraction duration than the conventional MSFHW configuration.

## 4. CONCLUSIONS

To improve geothermal recovery from abandoned reservoirs, we measured dynamic-fracture conductivity under reservoir conditions and derived a dynamic-fracture conductivity function. We then introduced the FCLG concept and built four models—GEE-FCLG, GEE-SFCLG, GEE-CLG, and GEE-MSFHW—to compare the FCLG (and its simplified one-fracture variant, SFCLG) against conventional CLG and MSFHW configurations. The main findings are:

The dynamic-fracture conductivity coefficient increases linearly with reservoir temperature and confining pressure, and increases exponentially with flow rate. The HFTTA and DFTTA frameworks invert bottom-hole temperature to track time-varying reservoir, hydraulic-fracture, and dynamic-fracture parameters during heat extraction; in DFTTA, the characteristic “peak-flow” signature captures the evolution of dynamic fractures.

Three proposed metrics—dynamic-fracture contraction coefficient, pressure-sensitivity coefficient, and flow-rate transmission coefficient—quantify how temperature, confining pressure, and flow rate, respectively, influence dynamic-fracture behavior in abandoned (geothermal) reservoirs. Among these factors, flow rate exerts the strongest effect.

The FCLG and its simplified SFCLG systems outperform conventional schemes. Relative to MSFHW, FCLG delivers ~1.7× higher heat-extraction efficiency, ~3× longer stable production, a maximum produced-temperature gain of 12.5–19.9 K, and a maximum net thermal-power increase of 8.9–9.4 MW. Even the SFCLG surpasses CLG, achieving ~2.27× higher efficiency, a 5.5–16.4 K rise in peak produced temperature, and a 2.25–3.6 MW boost in maximum net heat power.

Injection temperature is the dominant control on heat-extraction efficiency, followed by injection flow rate and then temperature difference. Lower injection temperatures, lower flow rates, and larger temperature differences enhance heat-extraction performance.


## ACKNOWLEDGEMENT

This research was supported by the Postdoctoral Fellowship Program (Grade B) of China Postdoctoral Science Foundation under Grant Number GZB20250681. This research was supported by Science Foundation of China University of Petroleum, Beijing (No.2462025XKBH025).


## REFERENCE


[1] Valentine SV. Emerging symbiosis: Renewable energy and energy security. Renewable and Sustainable Energy Reviews. 2011;15(9):4572-8.

[2] Tian X, You F. Carbon-neutral hybrid energy systems with deep water source cooling, biomass heating, and geothermal heat and power. Applied Energy. 2019;250:413-32.

[3] Aghahosseini A, Breyer C. From hot rock to useful energy: A global estimate of enhanced geothermal systems potential. Applied Energy. 2020;279:115769.

[4] Gudala M, Yan B, Tariq Z, Zhang F, Sun S. Doublet huff and puff: A new technology for efficient geological CO2 sequestration and stable geothermal recovery. Applied Energy. 2024;367:123349.

[5] Deng P, Chen Z, Peng X, Wang J, Zhu S, Ma H, et al. Optimized lower pressure limit for condensate underground gas storage using a dynamic pseudo-component model. Energy. 2023;285:129505.

[6] Wan Y, Yuan Y, Zhou C, et al. Multiphysics coupling in exploitation and utilization of geo-energy: State-of-the-art and future perspectives[J]. Advances in Geo-Energy Research, 2023, 10(1): 7-13.

[7] Ezekiel J, Ebigbo A, Adams BM, Saar MO. Combining natural gas recovery and CO2-based geothermal energy extraction for electric power generation. Applied Energy. 2020;269:115012.

[8] Weinand JM, Kleinebrahm M, McKenna R, Mainzer K, Fichtner W. Developing a combinatorial optimisation approach to design district heating networks based on deep geothermal energy. Applied Energy. 2019;251:113367.

[9] Buonomano A, Calise F, Palombo A, Vicidomini M. Energy and economic analysis of geothermal–solar trigeneration systems: A case study for a hotel building in Ischia. Applied Energy. 2015;138:224-41.

[10] Xue Z, Ma H, Sun Z, Lu C, Chen Z. Technical analysis of a novel economically mixed CO2-Water enhanced geothermal system. Journal of Cleaner Production. 2024;448:141749.

[11] Wan Y, Yuan Y, Zhou C, et al. Multiphysics coupling in exploitation and utilization of geo-energy: State-of-the-art and future perspectives[J]. Advances in Geo-Energy Research, 2023, 10(1): 7-13.
[12] Wu B, Zhang X, Jeffrey RG, Bunger AP, Jia S. A simplified model for heat extraction by circulating fluid through a closed-loop multiple-fracture enhanced geothermal system. Applied Energy. 2016;183:1664-81.
[13] Ziabakhsh-Ganji Z, Nick HM, Donselaar ME, Bruhn DF. Synergy potential for oil and geothermal energy exploitation. Applied Energy. 2018;212:1433-47.
[14] Tomac I, Sauter M. A review on challenges in the assessment of geomechanical rock performance for deep geothermal reservoir development. Renewable and Sustainable Energy Reviews. 2018;82:3972-80.
[15] Santos L, Dahi Taleghani A, Elsworth D. Repurposing abandoned wells for geothermal energy: Current status and future prospects. Renewable Energy. 2022;194:1288-302.
[16] Guo W, Deng S, Sun Y. Recent advances on shale oil and gas exploration and development technologies[J]. Advances in Geo-Energy Research, 2024, 11(2): 81-87.
[17] Wang Z, Ning Z, Guo W, Zhan J, Zhang Y. Study of fracture monitoring and heat extraction evaluation in geothermal reservoir modified by abandoned well pattern: Numerical models and case studies. Energy. 2024;296:131144.
[18] Cai J. AGER launches one-journal-one-forum mode to achieve a leading geo-energy exchange platform[J]. Advances in Geo-Energy Research, 2024, 13(2): 81-82.
[19] Sun F, Yao Y, Li G, Li X. Geothermal energy extraction in CO2 rich basin using abandoned horizontal wells. Energy. 2018;158:760-73.
[20] Templeton JD, Ghoreishi-Madiseh SA, Hassani F, Al-Khawaja MJ. Abandoned petroleum wells as sustainable sources of geothermal energy. Energy. 2014;70:366-73.
[21] Hu X, Banks J, Guo Y, Liu WV. Retrofitting abandoned petroleum wells as doublet deep borehole heat exchangers for geothermal energy production—a numerical investigation. Renewable Energy. 2021;176:115-34.
[22] Lu Z, Wang L, Guo Z, et al. The microfluidic in geo-energy resources: Current advances and future perspectives[J]. Advances in Geo-Energy Research, 2025, 16(2): 171-180..
[23] Kurnia JC, Putra ZA, Muraza O, Ghoreishi-Madiseh SA, Sasmito AP. Numerical evaluation, process design and techno-economic analysis of geothermal energy extraction from abandoned oil wells in Malaysia. Renewable Energy. 2021;175:868-79.
[24] Zhou Z, Jin Y, Zeng Y, Zhang X, Zhou J, Zhuang L, et al. Investigation on fracture creation in hot dry rock geothermal formations of China during hydraulic fracturing. Renewable Energy. 2020;153:301-13.
[25] Zhang C, Wang X, Jiang C, Zhang H. Numerical simulation of geothermal energy production from hot dry rocks under the interplay between the heterogeneous fracture and stimulated reservoir volume. Journal of Cleaner Production. 2023;414:137724.